Journal of Materials Chemistry B

ROYAL SOCIETY OF CHEMISTRY

PAPER

View Article Online
View Journal | View Issue

Check for updates

Cite this: J. Mater. Chem. B, 2023, 11, 4354

Dissolving microneedles based on ZnO nanoparticles and an ionic liquid as synergistic antibacterial agents†

Xiaodan Li, Wenzhen Du, Wenxin Xu, Guixia Ling* and Peng Zhang *

Received 20th January 2023,
Accepted 21st April 2023

DOI: 10.1039/d3tb00127j

rsc.li/materials-b

Published on 09 mai 2023. Downloaded on 2024-07-18 08:24:25.

The use of nanomaterials to replace antibiotics has developed rapidly in the past decade, among which zinc oxide nanoparticles (ZnO NPs) have been proven to exhibit antibacterial properties and low toxicity in the treatment of microbial infections, and have been applied in antibacterial agent preparation. However, one of the problems of ZnO NPs is that these particles do not disperse well in some media, which reduces their antibacterial effects. Ionic liquids (ILs) are a class of low melting point salts containing organic cations and organic/inorganic anions; they have good biocompatibility and can not only enhance the dispersion of ZnO NPs but also have antibacterial properties. Microneedles (MNs) are an emerging transdermal drug delivery platform, which can effectively establish a transport channel in the epidermis and deliver the drug to a predetermined depth without causing pain, skin damage or overstimulation. Dissolving microneedles (DMNs) have developed rapidly because of several advantages. In this study, it is verified that ZnO NPs dispersed in the imidazolidinyl IL exhibit excellent and enhanced antibacterial effects compared with single ZnO NPs and a single IL. Therefore, ZnO NPs/IL dispersion showed good antibacterial activity. Then, ZnO NPs/IL dispersions with synergistic antibacterial properties were used as antibacterial agents to prepare DMNs. *In vitro* antibacterial results showed that DMNs also had good antibacterial properties. Furthermore, DMNs were applied to treat wound infection. Antibacterial DMNs were inserted into the infected wound and then dissolved and released, resulting in microbial death and acceleration of wound healing.

1. Introduction

For a long time, a series of infectious diseases caused by bacteria have been a serious threat to global public health.[1,2] Antibiotics are the most commonly used drugs for treating bacterial infections.[3] However, with the abuse of antibiotics, antibiotic drugs cause a lot of waste, and the related drug resistance, adverse reactions and other hazards are becoming more and more serious.[4,5] Therefore, there is an urgent need for effective, durable and safe "ideal antimicrobials" (which do not involve antibiotics) to deal with increasingly complex and stubborn bacterial infectious diseases and overcome the disadvantages of traditional antibiotic therapy.[6] With the infiltration and continuous employment of nanotechnology in the development of antibacterial agents,[5] nanomaterials are gradually used to replace antibiotics. The development of and research on novel antimicrobial agents based on nanomaterials have developed rapidly in the last decade. In addition, ILs with antibacterial properties have also gradually attracted the attention of researchers in recent years.

ZnO NPs are widely used in the medicine and biomedical industry. The literature shows that nanometer ZnO exhibits bactericidal and bacteriostatic activity.[7,8] Moreover, compared with conventional compounds, metal oxide nanoparticles are more stable under extreme conditions and also exhibit antibacterial activity at low concentrations.[9] Meanwhile, ZnO NPs have the advantages of good biocompatibility and low toxicity.[10] At present, the antibacterial mechanisms of ZnO NPs have been proposed mainly as follows: direct contact between ZnO NPs and cells results in the loss of bacterial cell integrity;[11,12] ZnO NPs enter cells through diffusion or endocytosis, and interfere with the function of mitochondria after contact with the cytoplasm, promoting the release of ROS[13] and Zn^{2+},[14,15] which are able to penetrate cell membranes and reach DNA, causing nuclear damage and cell death.[16] However, one of the main disadvantages of using ZnO NPs as an antibacterial agent is that they have poor dispersion in general medium, reduced specific surface area and weakened surface activity, which results in decreased antibacterial performance of ZnO NPs. To achieve a better antibacterial effect, the increase of the concentration of ZnO NPs may pose a threat to normal and healthy cells.

Wuya College of Innovation, Shenyang Pharmaceutical University, No. 103, Wenhua Road, Shenyang 110016, China. E-mail: zhangpengspu@163.com, pharlab@163.com; Fax: +86-24-2398 6256; Tel: +86-24-2398 6256

† Electronic supplementary information (ESI) available. See DOI: https://doi.org/10.1039/d3tb00127j

This journal is © The Royal Society of Chemistry 2023

Published on 09 mai 2023. Downloaded on 2024-07-18 08:24:25.

Recently, a class of solvents called ILs have emerged as suitable dispersion media for various nanoparticles.[17] ILs generally refer to a variety of salts with the melting point below 100 °C and consist of defined anions and cations. ILs are pollution-free, recyclable, stable and non-volatile green solvents.[18,19] ILs have asymmetric ions with a delocalized electrostatic charge, which make them suitable as dispersion medium for metal nanoparticles, carbon nanotubes, cellulose, *etc.*[20] Electrostatic interactions occur when nanoparticles are dispersed in an IL. In these cases, clusters of positive and negative ions normally found in ILs surround the surface of the nanoparticles, rather than individual molecules like water, thus improving the dispersion of nanoparticles.[21] In addition, ILs exhibits an excellent antibacterial effect. Imidazole salt, piperidine salt, pyridine salt, pyrrole salt and other ILs possess the ability to inhibit the growth of pathogenic and non-pathogenic bacteria and fungi.[22] Imidazole ILs have a flexible, adjustable structure, and good water solubility. More importantly, imidazole cations can damage the integrity of bacterial membranes or damage intracellular DNA, which could lead to high efficiency and broad-spectrum antibacterial activity.[23] Therefore, ZnO NPs are dispersed in an IL to act as an antibacterial agent. On the one hand, both ZnO NPs and IL exhibit an antibacterial effect; on the other hand, ILs can improve the dispersion of ZnO NPs, and their combined use shows a synergistic bacteriostatic effect. ZnO NPs/IL dispersion can be used as an antibacterial agent, but its preparation as MNs has not been studied. Since the dispersion is in the liquid state and inconvenient when it is used as a skin antibacterial agent, it is a very appropriate choice to prepare it in the form of MNs for drug administration, and this design has not been reported in the literature to date.

In general, there are many ways to administer drugs for skin infections. Although topical or transdermal drug delivery systems are effective against superficial bacterial infections of the skin, most antimicrobials have poor permeability and cannot pass through the stratum corneum and epidermis resulting in insufficient effectiveness against subcutaneous microorganisms.[24] Subcutaneous injections can deliver drugs to the dermis or even subcutaneous tissues, but they cause problems such as pain, leading to poor compliance. The emerging MNs technology provides a continuous and controllable approach. MNs are a minimally invasive transdermal drug delivery system that can form micropores on the skin surface, which can deliver drugs or compounds to specific sites and predetermined depths[25,26] while reducing pain and tissue damage.[27] The transdermal drug delivery system of MNs reduces many of the challenges associated with injectable drug delivery systems. Antibacterial MNs can be used directly as a delivery platform against pathogens. There are several ways to load antimicrobial agents into MNs, including modifying the polymer matrix with antimicrobial agents such as quaternary ammonium salts; adding nano-antibacterial materials, such as Ag, ZnO or CuO NPs to the MNs; wrapping antibiotics/biomolecules directly in MNs.[28] MNs can be divided into solid, hollow, coated, dissolving, degradable and swelling MNs.[29] Different types of MNs have slightly different uses. Among them, DMNs have attracted much attention because of their advantages such as simple production, low cost, biodegradability and biocompatibility,[30] as well as drug release control.[31,32] However, the stability, mechanical strength and drug loading capacity of DMNs are major problems. DMNs are usually prepared from biodegradable and biocompatible polymers, including carbohydrates (hyaluronic acid, maltose, and chitosan)[33,34] and so on. These compounds can be modified and cross-linked to improve the stability and mechanical strength of DMNs. And the problem of low drug loading can be solved by developing antibacterial agents with better antibacterial effects.

In this study, the dispersibility and synergistic bacteriostatic performance of ZnO NPs in an IL were studied, and they were prepared in the form of DMNs as an antibacterial agent for treating wound infection *in vitro*. Methacrylate hyaluronic acid (MeHA) was prepared as the matrix of DMNs, and the DMNs were prepared through UV light crosslinking to improve their stability and mechanical strength. The DMNs were characterized and their antibacterial properties were investigated. The results showed that DMNs with different concentrations of ZnO NPs exhibited different antibacterial effects. Finally, the wound infection models were established and treated with DMNs, which achieved a good antibacterial effect and an improved healing effect.

2. Materials and methods

2.1. Materials

Hyaluronic acid (HA, M_w = 200–400 kDa) was obtained from Bloomage Biotechnology Co., Ltd. *N*,*N*-Dimethylformamide (DMF) was purchased from Tianjin Fuyu Fine Chemical Co., Ltd. Methacrylic anhydride was purchased from Shanghai Macklin Biochemical Co., Ltd. ZnO NPs (99.8%, 50 ± 10 nm), 1-butyl-3-methylimidazolium chloride (97%) and 1-hydroxycyclohexyl phenyl ketone (HCPK) were purchased from Shanghai Aladdin Biochemical Technology Co., Ltd. Mueller Hinton (MH) Broth was purchased from Haibo Biotechnology Co., Ltd. Agar (powder) was purchased from KERMEL. *S. aureus* and *E. coli* were purchased from Beijing Preservation Biotechnology Co., Ltd.

Sprague–Dawley (SD) rats were obtained from the Experimental Animal Center of Shenyang Pharmaceutical University. All animal experiments throughout the study were approved by the ethics committee of Shenyang Pharmaceutical University, China and conformed to the Guidelines for the Care and Use of Laboratory Animals published by the National Institutes of Health, USA. And the IACUC number is SYPU-IACUC-2022-0302-058.

2.2. Synthesis of MeHA

MeHA was synthesized according to the literature procedure with a slight modification.[35] Briefly, 2.0 g HA was fully dissolved in 100 mL of deionized water (DIW) and stirred overnight for complete dissolution. Then, 2/3 (v:v) of the water and DMF were added and stirred well. Methacrylic anhydride was added dropwise to the mixed solution at a ratio of 1/3 HA disaccharide unit/MA mole ratio. The pH of the solution was adjusted to pH 8–9 with 3 N NaOH. The reaction was maintained at 4 °C under continuous stirring for 24 hours. After

Published on 09 mai 2023. Downloaded on 2024-07-18 08:24:25.

stirring, the solution was transferred to a dialysis membrane (M_w = 14 kDa cut-off) and dialyzed for 3 days with DIW. Finally, the purified product was collected by lyophilization.

2.3. Preparation of ZnO NPs/IL dispersions

The IL used in this paper was 1-butyl-3-methylimidazolium chloride. Different concentrations of ZnO NPs were suspended in 10 mmol L^{-1} IL and subjected to ultrasonic treatment. Different amounts of water and times could provide different ultrasonic energy and affect the degree of dispersion. The particle sizes and polydispersity index (PDI) were measured on a Malvern laser particle size analyzer. The ZnO NPs dispersed in DIW were treated in the same way.

2.4. Bacterial culture

In this study, the antibacterial properties were tested by using Gram-negative *E. coli* and Gram-positive *S. aureus* as microbial models. *S. aureus* and *E. coli* bacteria were cultured in the MH liquid medium at 37 °C at the rate of 100 rpm for an appropriate time until they reached the exponential growth stage. The concentration of bacteria could be ensured by measuring the optical density at 600 nm wavelength (OD600). The OD600 value of the bacterial suspension was adjusted to 0.1 (equivalent to the concentration of 10^8 CFU mL^{-1}). Then the bacterial solution was diluted step by step to 10^6 CFU mL^{-1} for the bacteriostatic experiment.

2.5. Synergism analysis of ZnO NPs and IL

2.5.1. MIC and MBC. Minimum inhibitory concentration (MIC) is the lowest concentration that could inhibit the growth of bacteria. Minimum bactericidal concentration (MBC) is the lowest concentration that can kill bacteria in the medium. In this part, 50 μL of *E. coli* and *S. aureus* in the logarithmic phase at a concentration of 10^6 CFU mL^{-1} and 50 μL of the medium were added to each well of the 96-well plate, respectively, and then 100 μL of different concentrations of the ZnO NPs/DIW dispersion and different concentrations of IL were added, respectively. The final concentration of the ZnO NPs/DIW dispersion was 0.01, 0.02, 0.04, 0.08, 0.16, 0.32, and 0.64 mg mL^{-1}, and the final concentration of IL was 1, 2, 4, 8, 16, 32, and 64 mmol L^{-1}, and the blank control was set. The solution was incubated at 37 °C for 24 h. At the end of the culture, the OD value of each well was measured using a microplate reader. The concentration of the sample in the well with the OD value less than or equal to the blank control was the MIC of the sample against *E. coli* and *S. aureus*. 10 μL of each bacterial solution larger than the MIC was evenly coated on MH plates, and the plates were placed upside down in an incubator at 37 °C for 24 h. The minimum concentration of ZnO NPs/DIW and IL without colony growth was the MBC of ZnO NPs and IL against *E. coli* and *S. aureus*, respectively. The test was repeated three times.

2.5.2. Fractional inhibitory concentration (FIC) index. The study of synergism analysis was performed by the combined drug sensitivity test. 50 μL of *E. coli* and *S. aureus* in the logarithmic phase with a concentration of 10^6 CFU mL^{-1} and 50 μL of the medium were added to each well of the 96-well plate. Then different concentrations of ZnO NPs/DIW and IL were added to the horizontal and vertical columns of the 96-well plate by the checkerboard method according to section 2.5.1. The combinations of different concentrations of ZnO NPs/DIW and IL were placed in each well and mixed evenly with the bacterial solution, then cultured for 24 h at 37 °C in an incubator. Blank control was set under the same conditions. At the end of the culture, the absorbance value of each well was measured using the microplate reader. Similarly, the concentration of the combination in the well with the absorbance value less than or equal to the blank control was the MIC of the combination against the *E. coli* and *S. aureus*. The checkerboard test was repeated three times.

The FIC was calculated as the judgment basis for the combined drug sensitivity test. And the FIC was calculated based on the MIC of a single drug of two drugs and the MIC of the combination of two drugs. The calculation formula was as follows:

$$\mathrm{FIC} = \frac{\mathrm{MIC}_{A_{\mathrm{combination}}}}{\mathrm{MIC}_{A_{\mathrm{alone}}}} + \frac{\mathrm{MIC}_{B_{\mathrm{combination}}}}{\mathrm{MIC}_{B_{\mathrm{alone}}}}$$

FIC $\leq$ 0.5: synergy effect; 0.5 $<$ FIC $\leq$ 1: superimposition effect; FIC $>$ 1: antagonism effect.

2.5.3. Test of the antibacterial effect of ZnO/IL dispersions. The concentration of IL was set as 10 mmol L^{-1}, and the concentration of ZnO NPs was 0.09, 0.10, 0.11, 0.12, 0.13 mg mL^{-1}, respectively. Using *E. coli* and *S. aureus* as models, the antimicrobial activity of ZnO NPs/IL dispersions was detected by plate counting. The samples were co-cultured with the bacterial suspension (10^6 CFU mL^{-1}) in 96-well plates for 24 h at 37 °C. Then, 10 μL of diluted bacterial suspension was coated on MH plates and the number of colonies in each plate was observed after 24 h of culture at 37 °C. In order to ensure the reliability of the experiment, we did at least three experiments for each group (n = 3).

2.6. Fabrication of DMNs

MeHA (different concentrations) and HCPK (0.5 mg mL^{-1}) were mixed in the ZnO NPs/IL or ZnO NPs/DIW dispersions thoroughly and evenly. Then, 500 μL of the mixed pregel was loaded into the mold and centrifuged in a centrifuge at 3000 rpm for 10 min to remove air bubbles so that the mixed pregel would thoroughly fill the DMNs pinholes. After centrifugation, the molds were irradiated for 2 min under an ultraviolet lamp at a wavelength of 365 nm, then removed and dried for 24 h at room temperature. The DMNs were removed from the molds and dried at room temperature for 48 h and stored in a desiccator until further use. The preparation procedure of DMNs is shown in Fig. 1.

2.7. Characterization of DMNs

2.7.1. Morphological analysis. The morphology of the DMNs array was visualized with different instruments from different angles under different magnifications, including a camera, a digital optical microscope, and a scanning electron microscope (SEM). Each DMN consisted of 121 (11 × 11) complete and continuous needle arrays, and each needle was in the shape of a quadrangular pyramid, 800 μm high and 410 μm wide at the base, and spaced 800 μm apart. In addition, the dispersion of ZnO

 This journal is © The Royal Society of Chemistry 2023

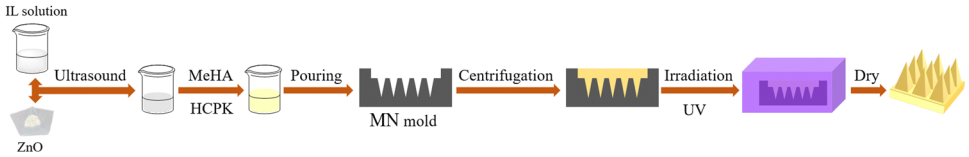

Fig. 1 The preparation procedure of DMNs.

Published on 09 mai 2023. Downloaded on 2024-07-18 08:24:25.

NPs throughout the DMNs prepared by ZnO NPs/IL dispersions had also been observed by SEM compared with the DMNs prepared by ZnO NPs/DIW dispersions.

2.7.2. Mechanical properties. The mechanical strength of DMNs was tested by mechanical compression using a universal testing machine (CMT6103).

2.7.3. Skin insertion test and skin healing test *in vitro*. To evaluate the efficacy of the DMNs in penetrating the skin, the pigskin was used for tests as an alternative to human skin.[36] The pigskin was rinsed with normal saline and then dried with filter paper. The skin was then spread on the filter paper with the dermis facing downward. The DMNs were inserted into the skin by thumb pressure being applied for 30 s. Then the DMNs were pulled out. The insertion of the skin after piercing of pigskin by DMNs were observed and the healing of the insertion site at different time was recorded. In order to make the insertion holes visible at the patch application site, 0.2% trypan blue solution was applied to the application site and left for 5 min. PBS solution was then used to wash out the trypan blue solution and the skin surface was dried using filter paper. The stained blue holes that appeared at the site of insertion on the skin surface were photographed and recorded. Then the holes left on the surface of the pig skin were counted, and the insertion rate was calculated (the higher the insertion rate, the better the mechanical properties). The insertion rate was calculated according to the following formula:

$$\text{Insertion rate}\,(\%) = \frac{\text{Number of microholes appeared}}{\text{Number of needles per DMNs}\,(11\times 11)} \times 100\%$$

2.7.4. Skin puncture test and skin healing test *in vivo*. To further explore the puncture ability of DMNs, a skin puncture test was carried out on rat skin. And the healing of micropores after the insertion of DMNs in live rats could be observed at the same time. After 14 days of normal feeding of SD rats, the hair removal ointment was evenly applied to the back skin of the rat for 5 min. The depilatory cream and hair on the back of the rat were wiped off with warm water and the back skin of the rat was observed. When the rat skin was in good condition, the DMNs were inserted vertically into the back skin of the rat with an appropriate force and the DMNs were removed after 30 s. The puncture of the skin and the healing process were recorded with a camera. The healing of micropores on the skin surface of the rat was observed at 2 min, 5 min and 10 min.

2.7.5. Dissolution study of DMNs. DMNs were vertically inserted into the skin of live rats and removed after maintaining for different times. The remaining needles on DMNs were observed under a light microscope to evaluate the dissolving behaviors of the MNs *in vivo*.

2.8. Antibacterial ability test of DMNs

2.8.1. Co-culture. DMNs with an IL concentration of 10 mmol L^{-1} and ZnO NPs concentrations of 0.12, 0.24, 0.36, and 0.48 mg mL^{-1} were prepared according to the method described in section 2.4. The antibacterial activity of DMNs was also detected by the plate counting method. $\frac{1}{4}$ of the DMNs were added to 100 μL of bacterial suspension (10^6 CFU mL^{-1}), and 500 μL of normal saline was added to prevent DMNs from not being completely dissolved and release antibacterial agents. The mixture was co-cultured for 24 hours at 37 °C in a 48-well plate. Then, diluted bacterial suspension was coated on MH plates. The number of colonies in each dish was observed after 24 h of incubation at 37 °C. In order to ensure the reliability of the experiment, we did at least three experiments for each group ($n = 3$).

2.8.2. Growth curve. The growth curves of DMNs against *S. aureus and E. coli* with different concentrations were measured using a microplate reader at different times. $\frac{1}{2}$ of the DMNs were added to 400 μL of bacterial suspension (10^8 CFU mL^{-1}), and 800 μL of normal saline was added to prevent DMNs from not being completely dissolved and release antibacterial agents. The control group had only bacteria-containing cultures. In order to ensure the reliability of the experiment, we repeated the experiments three times for each group ($n = 3$).

2.9. Blood compatibility test

The procedure for the hemolysis assay of DMNs followed the published methods.[37] The pregel for making DMNs was prepared, and then the DMNs pregel loaded with different concentrations of ZnO NPs was leached with physiological saline to obtain leaching solutions, respectively, then the leaching solution was passed through a 0.22 μm filter. Then, the solution after filtration was incubated with rat red blood cells (RBC, 2% v/v) for 1 h at 37 °C. The physiological saline-treated suspension was used as a negative control, while the suspension treated with DIW was used as a positive control. Three replicate samples were provided for each group. After incubation, the samples were centrifuged at 13,000 rpm for 5 min, and the OD value of the supernatant was measured at 545 nm. The formula for calculating the hemolysis rate was as follows:

$$\text{Hemolysis ratio}\,(\%) = \frac{\text{OD}_{\text{sample}} - \text{OD}_{\text{negative}}}{\text{OD}_{\text{positive}} - \text{OD}_{\text{negative}}} \times 100\%$$

2.10. Wound healing experiment

To further investigate the practical value of DMNs for antibacterial, we established infected cutaneous defect rat models. Rats were depilated. A wound was cut with an area of about 1 cm^2 on the skin of the back of the rats. 10 μL of the bacterial

Published on 09 mai 2023. Downloaded on 2024-07-18 08:24:25.

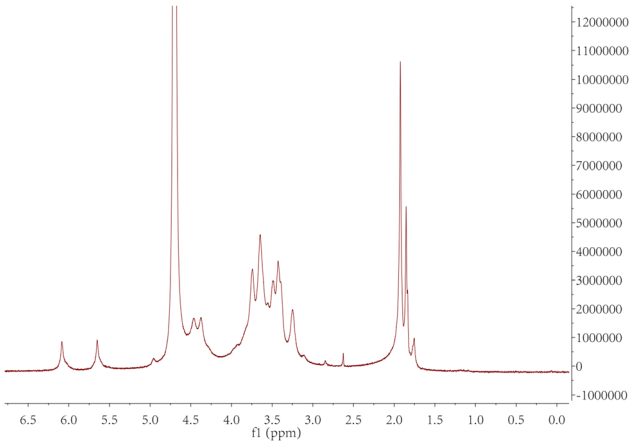

Fig. 2 ^{1}H-NMR of MeHA.

solution of *S. aureus* (10^{8} CFU mL^{-1}) was applied to the wound for 1 min, and then scrubbed with normal saline for 1 min to complete the establishment of the wound model. The rats without DMNs treatment were used as the control group, and the rats treated with DMNs with ZnO NPs concentration of 0.48 mg mL^{-1} were used as the experimental group (n = 3). All rats were reared under the same conditions, and the wounds were photographed on different days. The healing rate of different days was calculated according to the area of the wound. Wound healing was determined by the healing rates and H&E staining at the wound site on day 15. The formula for the healing rate was as follows:

$$\text{Healing rate } (100\%) = \frac{S_0 - S_t}{S_0} \times 100\%$$

S_0 is the wound area on day 0; S_t is the wound area on day t.

3. Results

3.1. Characterization of MeHA

The purified product was obtained by lyophilization and characterized by ^{1}H-NMR spectroscopy (Fig. 2). The degree of modification was determined to be 22% by integration of methacrylate proton signals at 6.1 and 5.7, to the peak at 1.9 ppm related to the *N*-acetyl glucosamine of HA. MeHA: ^{1}H-NMR (D_2O, 600 MHz, δ ppm): 1.80–1.96 (m, 3H, CH_2═C(CH_3) CO), 1.99 (s, 3H, NHCOCH_3), 5.74 (s, 1H, CH_1H_2═C(CH_3) CO), 6.17 (s, 1H, CH_1H_2═C(CH_3) CO). The formula for the degree of modification is as follows:

$$\text{Graft degree } (\%) = \frac{\text{A}(6.1 \text{ ppm}) + \text{A}(5.7 \text{ ppm})}{\text{A}(1.9 \text{ ppm})} \times \frac{3}{2} \times 100\%$$

3.2. Characterization of ZnO/IL dispersions

Through using different amounts of water and time for ultrasonication, 2000 mL of water and 5 min were selected for the ultrasonication of the dispersion (Table S1, ESI†). In order to analyze the dispersion of ZnO NPs in IL, we measured the size of the nanoparticles at different concentrations and different solutions. The variations in the PDI of ZnO NPs were also measured. In Fig. 3, in terms of sizes and PDI, the dispersion of ZnO NPs in IL was smaller than that in DIW, which suggested that ZnO NPs dispersed in IL had much better dispersibility and a larger surface area.

3.3. Synergism analysis of ZnO NPs and IL

3.3.1. MIC and MBC. The MIC and MBC of ZnO NPs and IL against *E. coli* and *S. aureus* are shown in Table 1. The MBC/MIC ratio can be used to evaluate the bactericidal potential of antibiotics. If MBC/MIC is less than or equal to 4, antibacterial agents are considered to be bactericidal.[38] In this study, the MBC/MIC of ZnO NPs and IL were all less than 4, which proved that ZnO NPs and IL had bactericidal activity rather than inhibitory activity.

3.3.2. FIC. The MIC of the combination of ZnO NPs and IL are shown in Table 2 through the checkerboard method. According to the formula in section 2.8, the FIC values of ZnO NPs and IL for *E. coli* and *S. aureus* were calculated, which were $\frac{1}{2}$ and 3/8, respectively. According to the FIC calculation results the values were all less than or equal to 0.5, and it could be judged that ZnO NPs and IL had a synergistic antibacterial effect.

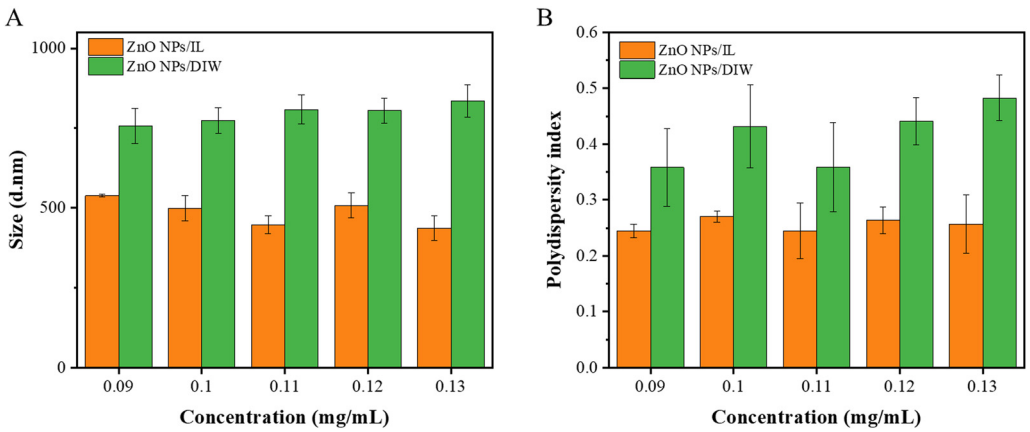

Fig. 3 Sizes and PDIs of ZnO NPs/IL and ZnO NPs/DIW with different concentrations (A) sizes; (B) PDIs.

 This journal is © The Royal Society of Chemistry 2023

Published on 09 mai 2023. Downloaded on 2024-07-18 08:24:25.

Table 1 The MIC and MBC of ZnO NPs and IL for *E. coli* and *S. aureus*

	E. coli		*S. aureus*	
	MIC	MBC	MIC	MBC
ZnO NPs (mg mL^{-1})	0.16	0.64	0.08	0.32
IL (mmol L^{-1})	8	16	8	16

3.3.3. Antibacterial effect of ZnO NPs/IL dispersions. The results of *E. coli* and *S. aureus* incubated with ZnO NPs/IL dispersions with different concentrations of ZnO NPs are shown in Fig. 4. The concentration of IL was fixed between MIC and MBC which was 10 mmol L^{-1}, and the concentration of ZnO NPs was 0.09, 0.10, 0.11, 0.12, and 0.13 mg mL^{-1}, respectively. According to the results of the combined drug sensitivity test of ZnO NPs and IL, it could be found that when the concentration of IL was fixed between MIC and MBC, the concentration of corresponding ZnO NPs of ZnO NPs/IL dispersions decreased when reaching the bactericidal effect compared with the MBC of ZnO NPs. For *E. coli*, no colonies were found in ZnO NPs/IL dispersions with ZnO NPs concentrations above 0.12 mg mL^{-1}, and for *S. aureus*, no colonies were found in ZnO NPs/IL dispersions with ZnO NPs concentrations above 0.10 mg mL^{-1} which were far less than the MBC of ZnO NPs for *E. coli* and *S. aureus*, respectively. Thus, it could be seen that ZnO NPs and IL had a synergistic antibacterial effect.

From MIC and MBC, FIC and antibacterial effect of ZnO NPs/IL dispersions, it was not difficult to see that ZnO NPs and IL had synergistic antibacterial ability. In addition, the antibacterial performance of ZnO NPs/IL dispersions against *S. aureus* was better than that of *E. coli* which is due to the difference between ZnO NPs against two kinds of bacteria. The reason for this result may be that the cell wall structure and surface chemical composition of *E. coli* and *S. aureus* are different. The cell wall structure of *E. coli* is complex, with an outer wall layer and an inner wall layer, and the outer wall layer is divided into three layers, while the cell wall structure of *S. aureus* is relatively simple, with only one layer. Therefore, for *E. coli*, the active antibacterial Zn^{2+} can penetrate *S. aureus* more easily. On the other hand, it may be because the high concentration of Zn^{2+} inhibits the growth of *E. coli* and *S. aureus*, while the low concentration of Zn^{2+} promotes the growth of *E. coli*.[39,40] Overall, the combination of ZnO NPs and IL had an excellent synergistic antibacterial effect and could be used as an antibacterial agent.

Table 2 The MIC and FIC of the combination of ZnO NPs and IL against the *E. coli* and *S. aureus*

	MIC		
	ZnO NPs (mg mL^{-1})	IL (mmol L^{-1})	FIC
E. coli	0.04	2	1/2
S. aureus	0.02	1	3/8

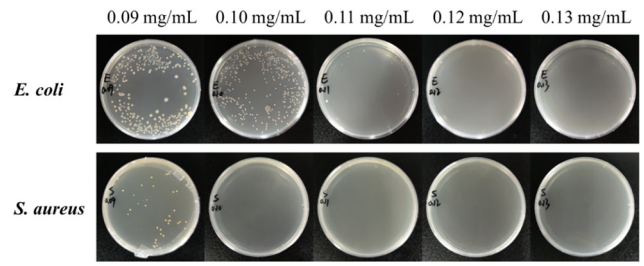

Fig. 4 Colony photos of *E. coli* and *S. aureus* incubated with ZnO NPs/IL dispersions with different concentrations of ZnO NPs.

3.4. Characterization of DMNs

3.4.1. Morphological representation. The structures of the prepared DMNs were microscopically analyzed using a camera, optical microscopy and SEM. As shown in Fig. 5, it could be seen from the images taken by the camera that the prepared DMNs had a square structure, complete backing, and neatly arranged needle tips. The DMN tips were observed from different angles under an optical microscope with complete tip morphology and uniform distribution. The magnified microstructure of the prepared MNs was further observed by SEM which showed that the surface of the tips was intact without pores. According to the obtained images, it could be seen that the prepared DMNs had an obvious quadrangular pyramid needle tip structure and good needle shape, indicating that the selected matrix prescription could produce DMNs with good morphology. At the same time, the dispersion degree of

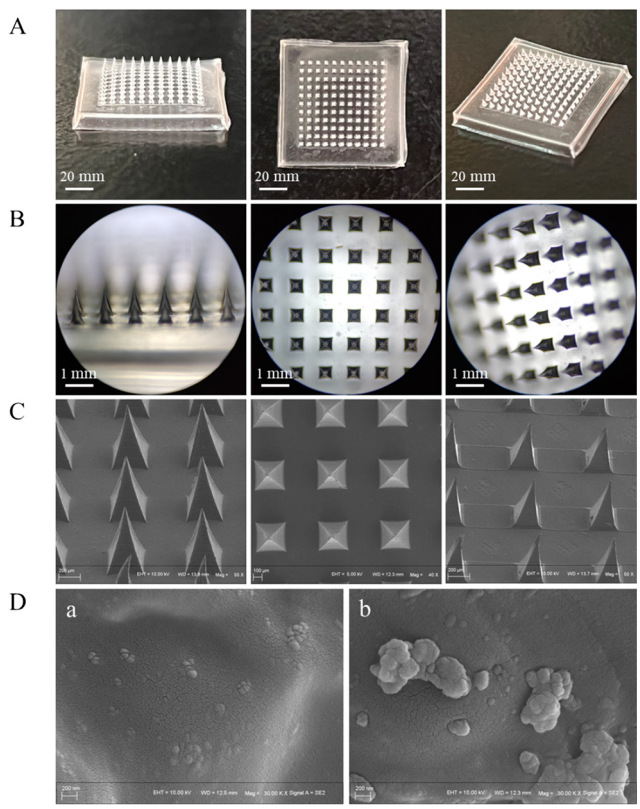

Fig. 5 Morphological characterization images of DMNs. (A) € direct view of the DMNs taken by the camera; (B) the shape of the DMN tips under an optical microscope; (C) the SEM images of DMNs; and (D) images of the dispersion of ZnO NPs in DMNs by SEM (a, DMNs based on ZnO NPs/IL; b, DMNs based on ZnO NPs/DIW).

Published on 09 mai 2023. Downloaded on 2024-07-18 08:24:25.

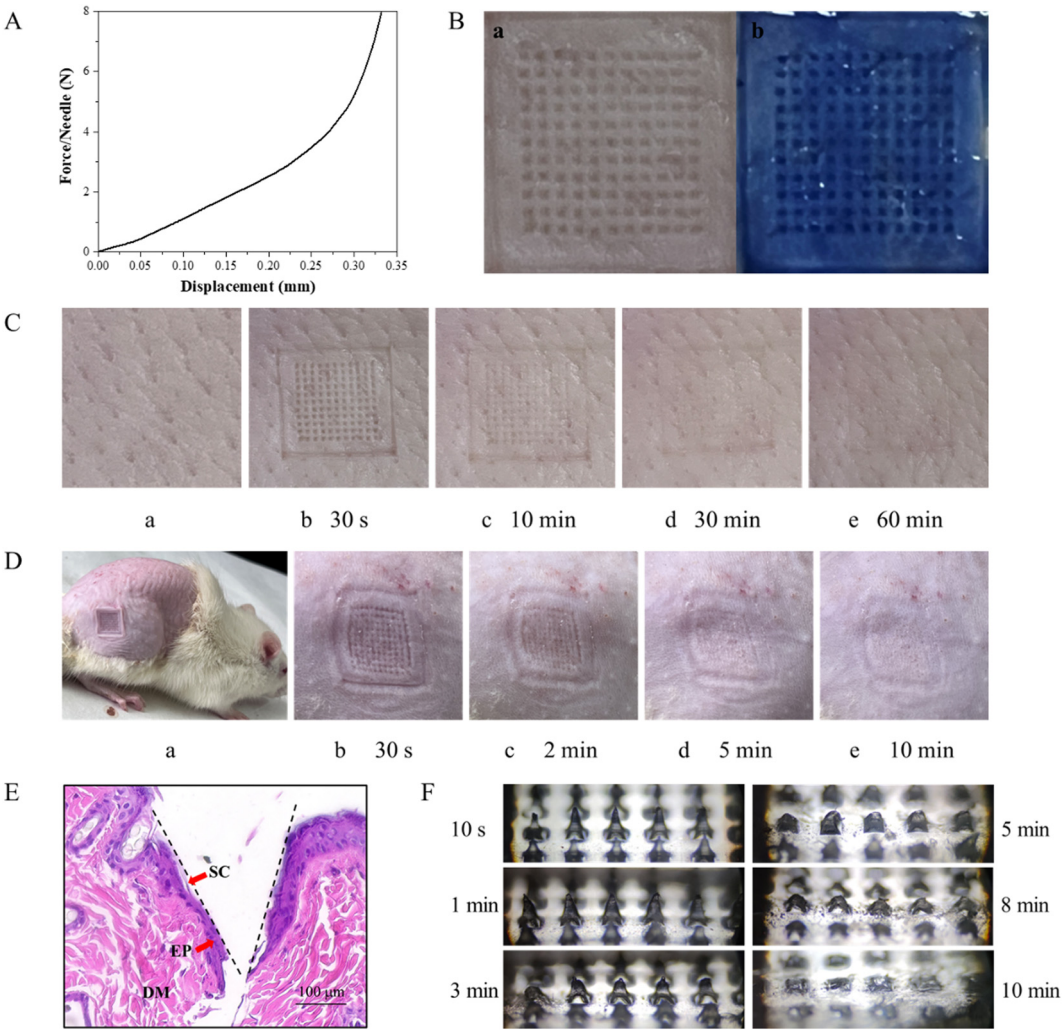

Fig. 6 (A) Mechanical behaviour of the DMNs; (B) the state of the holes left after DMNs were inserted into pigskin (a, original; b, stained); (C) the surface of pigskin treated with DMNs at different times; (D) skin healing process after DMN insertion into the dorsal skin of rats; (E) the H&E staining of the back skin of the rat that was punctured; and (F) the dissolution of DMNs in rat skin.

ZnO NPs in DMNs was also observed by SEM. In Fig. 5D, compared with the DMNs prepared by ZnO NPs/DIW dispersions, the ZnO NPs dispersed in IL more evenly, which indicated that the IL could enhance the dispersion of ZnO NPs.

3.4.2. Mechanical properties. As shown in Fig. 6A, using a universal testing machine, the tips of DMNs underwent continuous deformation, and the pressure on DMNs increased with the shape variable of the tips. When the shape variable of the tips was 0.23 mm, the pressure on the DMNs was about 3 N. It showed that DMNs could withstand a large force before deformation which indicated that DMNs had strong mechanical strength.

3.4.3. Skin insertion test and skin healing test *in vitro*. It could be seen from the figure that the pinholes formed by the DMNs piercing the pig skin after trypan blue staining were clearly visible (Fig. 6B). Then the holes left on the surface of the pig skin were counted, and the insertion rate was calculated to be about 99% according to the formula mentioned in section 2.5.2, indicating that the DMNs had good mechanical properties.

The DMNs were inserted into the skin by thumb pressure being applied for 30 s. The changes in the microchannels on the skin surface of the pig skin were observed after 30 s, 10 min, 30 min and 60 min, respectively. As shown in Fig. 6C, after the DMNs were removed for 30 min, the microchannels on the surface of the pigskin could still be observed, which proved that the DMNs could penetrate the skin successfully and had good mechanical strength. And at 60 min, the micropores were barely visible, indicating the healing time of DMNs in pigskin *in vitro* was 60 min.

3.4.4 Skin puncture test and skin healing test *in vivo*. The puncture ability and healing properties of DMNs were further investigated on the dorsal skin of rats. The results showed that DMNs could puncture the dorsal skin of rats, which suggested that DMNs had good puncture ability, and with the prolongation of time, the pores formed by the DMNs in the skin gradually healed and disappeared within 10 min (Fig. 6D). And no adverse reactions such as redness, swelling, and inflammation were observed on the skin surface of rats. In addition, it could be

 This journal is © The Royal Society of Chemistry 2023

Published on 09 mai 2023. Downloaded on 2024-07-18 08:24:25.

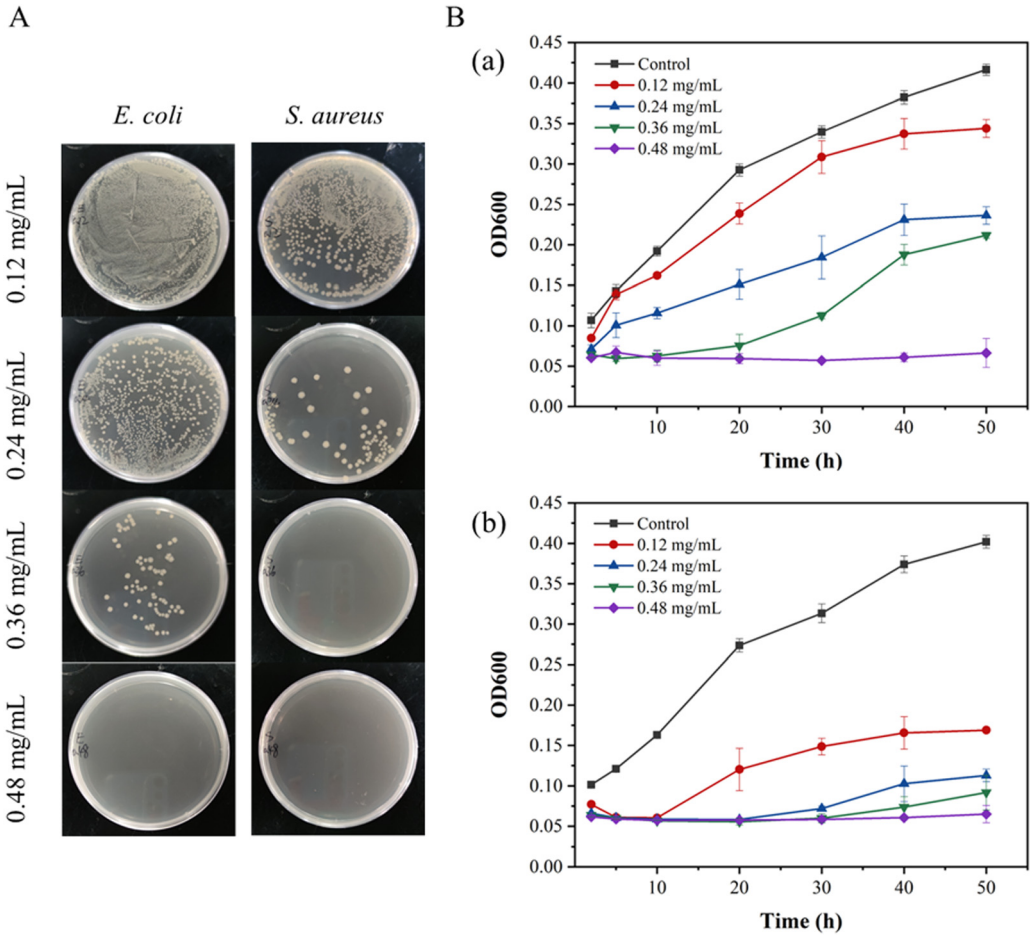

Fig. 7 (A) Colony photos of *E. coli* and *S. aureus* after incubation with DMNs with different concentrations of ZnO NPs; and (B) the growth curves of DMNs against *E. coli* (a) and *S. aureus* (b).

seen from H&E staining of the back skin of rats that was punctured (Fig. 6E) that DMNs successfully punctured the stratum corneum and epidermis to form micropores, but did not penetrate the dermis to the subcutaneous tissue, further indicating that DMNs had good skin puncture ability. At the same time, no hemorrhagic sites, necrotic tissues, and inflammatory factors were found in the H&E staining, indicating that DMNs would not cause some side effects while puncturing the skin, and the healing condition was good.

3.4.5. Dissolution study. In order to investigate the solubility of DMNs, dissolution experiments were carried out *in vivo*. The dissolution of the DMNs tips after insertion into the rat had different lengths at different times (Fig. 6F). From the results of the optical microscope images, the DMNs could be dissolved within 10 min after being inserted into the intact rat skin. It could be seen that DMNs could dissolve and achieve local administration rapidly.

3.5. Antibacterial ability test of DMNs

3.5.1. Co-culture. The DMNs with different concentrations of ZnO NPs were co-cultured with the bacterial solution, and the results are shown in Fig. 7A. For *E. coli*, no colonies were found after incubation with DMNs with ZnO NPs concentrations above 0.48 mg mL^{-1}, and for *S. aureus*, no colonies were found after incubation with DMNs with ZnO NPs concentrations above 0.36 mg μL^{-1}, respectively. In the same way, the antibacterial performance of the DMNs against *S. aureus* was better than that of *E. coli*. The increased ZnO NPs concentration might be due to the low ZnO NPs content and dissolution release of individual DMNs. Overall, DMNs showed good antibacterial properties.

3.5.2 Growth curve. Growth curves were performed by immersing DMNs in *E. coli* and *S. aureus* bacterial solutions to further evaluate the antibacterial properties of DMNs (Fig. 7B). From the results, DMNs with different concentrations had certain antibacterial effects compared with the control group, but the antibacterial effects were very different. With the increase of ZnO NPs concentration, the antibacterial effect was enhanced. For the two strains, different concentrations of DMNs also had different antibacterial effects. For *E. coli*, the four concentrations of DMNs had significant differences in antibacterial effects. Within 20 h, DMNs in which the concentrations of ZnO NPs were 0.36 mg mL^{-1} and 0.48 mg mL^{-1} had good antibacterial effects, but beyond 20 h, only 0.48 mg mL^{-1} DMNs showed strong antibacterial effects. For *S. aureus*, only 0.12 mg mL^{-1} concentration of DMNs had no significant antibacterial effect, and other concentrations of DMNs had a

Published on 09 mai 2023. Downloaded on 2024-07-18 08:24:25.

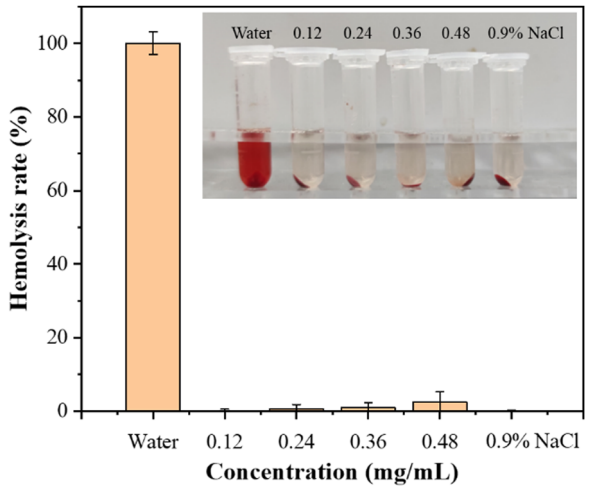

Fig. 8 The hemolysis rate of DMNs with different concentrations of ZnO NPs.

better antibacterial effect. But, within 50 h, only 0.48 mg mL^{-1} concentration of DMNs had strong antibacterial effects.

The results of antibacterial experiments showed that different concentrations of DMNs showed different antibacterial properties. It could be seen that it was dependent on the concentration of ZnO NPs. The higher the concentration of ZnO NPs, the higher the content of ZnO NPs in the prepared DMNs, the better the antibacterial performance. Therefore, for high microbial concentration infection, the problem could be solved by increasing the concentration of ZnO NPs and IL without affecting the mechanical strength of DMNs. However, an excessive increase in concentration may result in some side effects, so for ultra-high microbial concentration infection, it could be solved by adding a third antibacterial drug or increasing the frequency of administration. And the antibacterial results of ZnO NPs/IL dispersions and DMNs showed that ZnO NPs/IL had different antibacterial effects on the two kinds of bacteria. This might be due to different antibacterial effects of ZnO NPs on the two bacteria, which could be seen from the MIC and MBC of ZnO NPs and IL.

3.6. Blood compatibility test

To evaluate the blood compatibility of the prepared DMNs, a hemolysis experiment was performed. After incubating the analytes with red blood cells at 37 °C for 1 h, centrifuging the mixture at 13 000 rpm for 5 min, and measuring the OD value of the supernatant at 545 nm, the hemolysis rate was calculated. The results showed that the hemolysis rate of each experimental group was far less than 5%, indicating that the antibacterial DMNs had good blood compatibility. The hemolysis rate of DMNs is shown in Fig. 8.

3.7. Wound healing experiment

In the wound healing process, the changes of the wound were photographed and measured on 0, 2, 4, 6, 8, 10 and 12 days, as

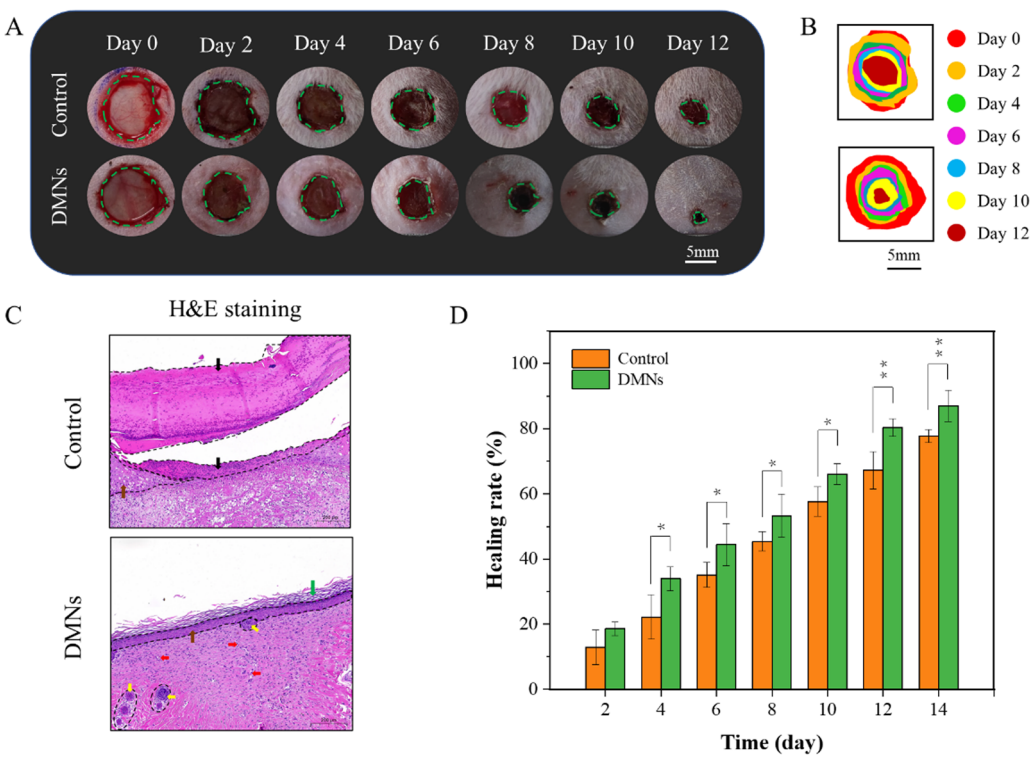

Fig. 9 (A) Wound images of the control and experimental group on days 0, 2, 4, 6, 8, 10 and 12; (B) schematic diagram of wound size in the two groups during the experimental time; (C) the H&E staining of the wounds (black arrow mean necrotic tissue; brown arrows mean new epidermal; green arrow means new stratum corneum; yellow arrows mean folliculus pilis; red arrows mean new blood vessels); and (D) the wound healing rate of the two groups (*$p < 0.1$, **$p < 0.05$).

 This journal is © The Royal Society of Chemistry 2023

Published on 09 mai 2023. Downloaded on 2024-07-18 08:24:25.

shown in Fig. 9A and B. Generally, the wounds on the back of the rats were nearly healed after 12 days with DMN treatment, while the wounds showed a slower healing rate in the control group (Fig. 9C). Moreover, from the fourth day, the healing rate of the experimental group was significantly different from that of the control group. In addition, it could be seen from the H&E staining that there were still a lot of necrotic tissue in the wound of the control group, but there were epidermis, stratum corneum, folliculus pilis and blood vessels in the group with DMNs treatment. These results all confirmed that DMNs with ZnO NPs/IL dispersion had a good antibacterial effect so that DMNs could promote wound healing.

4. Conclusion and outlook

In this study, the dispersion of ZnO NPs in an IL was first discussed, and then the synergistic antibacterial performance of ZnO NPs and the IL was explored. The results showed that ZnO NPs and the IL exhibited a synergistic antibacterial effect. In addition, compared with ZnO NPs/DIW, when the concentration of the IL was fixed between MIC and MBC, the concentration of ZnO NPs in ZnO NPs/IL dispersions greatly reduced, which also showed that ZnO NPs/IL exhibited an enhanced antibacterial effect and achieved a synergistic antibacterial effect. This was mainly because ZnO NPs showed good dispersion in the IL, which increased the specific surface area of ZnO NPs and the surface activity. Then ZnO NPs/IL was prepared in the form of DMNs. MeHA was successfully prepared and DMNs were successfully prepared using MeHA through UV light crosslinking. The prepared drug-loaded DMNs were characterized and the antibacterial properties were investigated. The integrity of the prepared DMNs could be seen by the appearance of the DMNs. The *In vivo* puncture ability test indicated that DMNs had good puncture ability. And DMNs could dissolve and release antibacterial agents in a short time. The antibacterial properties of DMNs were investigated by co-culture and growth curve experiments. The results showed that DMNs with 0.48 mg mL^{-1} ZnO NPs of ZnO NPs/IL dispersions exhibited strong antibacterial properties. Finally, the wound infection models were established. The healing speed of wounds with DMNs treatment was significantly faster, which indicated that DMNs had a good antibacterial effect.

The advantages of ZnO NPs/IL dispersions as composite antibacterial agents to prepare DMNs were mainly in the following aspects. According to its synergistic antibacterial performance, ZnO NPs/IL dispersions could achieve better antibacterial effect while reducing the amount of ZnO NPs and IL, thus avoiding the problem caused by increasing antibacterial activity of a single drug by increasing the dosage. But the liquid state and instability of ZnO NPs/IL dispersions were not conducive to the application of a skin antibacterial agent, so in this study, for the first time, ZnO NPs/IL dispersions were used as antibacterial agents to prepare DMNs as a skin antibacterial agent, making it convenient for treatment. DMNs faced some problems such as low mechanical strength, stability and drug loading. In this study, MeHA was synthesized as the substrate of DMNs and DMNs were prepared by the UV light crosslinking method which solved the mechanical strength and stability problems of DMNs. At the same time, the problem of low drug loading of DMNs was solved by developing antibacterial agents with synergistic antibacterial effects, such as ZnO NPs/IL dispersions. In general, the DMNs prepared using ZnO NPs/IL dispersions in this study showed a synergistic antibacterial effect, which provided enlightenment for the development of ''ideal antimicrobials''. As for antibacterial MNs, they are still in the initial development stage, so there is lot of space for future clinical research. There are several other factors that can be considered when designing antibacterial MNs in the future. For example, the size and shape of antibacterial MNs can be fine-tuned according to the characteristics of the infected sites. The geometry of the antibacterial MNs can also be adjusted to further facilitate their application. Drugs that promote tissue regeneration can also be added to antibacterial MNs to further promote wound healing.

Author contributions

Xiaodan Li: investigation, conceptualization, methodology, formal analysis, writing – original draft, and writing – review & editing; Wenzhen Du: writing – review & editing and validation; Wenxin Xu: writing – review & editing; Guixia Ling: resources. Peng Zhang: resources, writing – review & editing, and supervision.

Conflicts of interest

The authors declare that they have no known competing financial interests.

References

1 A. Gupta, S. Mumtaz, C.-H. Li, I. Hussain and V. M. Rotello, *Chem. Soc. Rev.*, 2019, **48**, 415–427.
2 Y. Liu, L. Shi, L. Su, H. C. van der Mei, P. C. Jutte, Y. Ren and H. J. Busscher, *Chem. Soc. Rev.*, 2019, **48**, 428–446.
3 D. L. Paterson and P. N. Harris, *Lancet Infect. Dis.*, 2016, **16**, 132–133.
4 M. O. Sommer and G. Dantas, *Curr. Opin. Microbiol.*, 2011, **14**, 556–563.
5 J. M. V. Makabenta, A. Nabawy, C. H. Li, S. Schmidt-Malan, R. Patel and V. M. Rotello, *Nat. Rev. Microbiol.*, 2021, **19**, 23–36.
6 B. Chen, F. Li, X. K. Zhu, W. Xie, X. Hu, M. H. Zan, X. Li, Q. Y. Li, S. S. Guo, X. Z. Zhao, Y. A. Jiang, Z. Cao and W. Liu, *Biomater. Sci.*, 2021, **9**, 826–834.
7 M. Khatami, R. S. Varma, N. Zafarnia, H. Yaghoobi, M. Sarani and V. G. Kumar, *Sustainable Chem. Pharm.*, 2018, **10**, 9–15.
8 V. A. Spirescu, R. Suhan, A.-G. Niculescu, V. Grumezescu, I. Negut, A. M. Holban, O.-C. Oprea, A. C. Birca, B. S. Vasile, A. M. Grumezescu, L. E. Bejenaru, G. D. Mogosanu,

Published on 09 mai 2023. Downloaded on 2024-07-18 08:24:25.

C. Bejenaru, P. C. Balaure, E. Andronescu and L. Mogoanta, *Nanomaterials*, 2021, **11**.
9 A. Krol, P. Pomastowski, K. Rafinska, V. Railean-Plugaru and B. Buszewski, *Adv. Colloid Interface Sci.*, 2018, **254**, 100.
10 A. Singh, N. B. Singh, S. Afzal, T. Singh and I. Hussain, *J. Mater. Sci.*, 2018, **53**, 185–201.
11 B. Ahmed, F. Ameen, A. Rizvi, K. Ali, H. Sonbol, A. Zaidi, M. S. Khan and J. Musarrat, *ACS Omega*, 2020, **5**, 7861–7876.
12 B. L. da Silva, B. L. Caetano, B. G. Chiari-Andreo, R. C. Linhari Rodrigues Pietro and L. A. Chiavacci, *Colloids Surf., B*, 2019, **177**, 440–447.
13 K. R. Raghupathi, R. T. Koodali and A. C. Manna, *Langmuir*, 2011, **27**, 4020–4028.
14 J. Pasquet, Y. Chevalier, E. Couval, D. Bouvier and M.-A. Bolzinger, *Int. J. Pharm.*, 2015, **479**, 88–95.
15 W.-S. Cho, R. Duffin, S. E. M. Howie, C. J. Scotton, W. A. H. Wallace, W. MacNee, M. Bradley, I. L. Megson and K. Donaldson, *Part. Fibre Toxicol.*, 2011, **8**.
16 W. Jiang, H. Mashayekhi and B. Xing, *Environ. Pollut.*, 2009, **157**, 1619–1625.
17 Z. He and P. Alexandridis, *Phys. Chem. Chem. Phys.*, 2015, **17**, 18238–18261.
18 X. Chao, C. Zhang, X. Li, H. Lv, G. Ling and P. Zhang, *Biomater. Sci.*, 2022, **10**, 1008–1017.
19 X. Li, N. Ma, L. Zhang, G. Ling and P. Zhang, *Int. J. Pharm.*, 2022, **612**, 121366.
20 K. S. Egorova, E. G. Gordeev and V. P. Ananikov, *Chem. Rev.*, 2017, **117**, 7132–7189.
21 A. Aditya, S. Chattopadhyay, D. Jha, H. K. Gautam, S. Maiti and M. Ganguli, *ACS Appl. Mater. Interfaces*, 2018, **10**, 15401–15411.
22 M. Sundararaman, R. Rajesh Kumar, P. Venkatesan and A. Ilangovan, *J. Med. Microbiol.*, 2013, **62**, 241–248.
23 R. Rossi and M. Ciofalo, *Molecules*, 2020, **25**.
24 A. J. Duplantier and M. L. van Hoek, *Front. Immunol.*, 2013, **4**, 143.
25 T. Waghule, G. Singhvi, S. K. Dubey, M. M. Pandey, G. Gupta, M. Singh and K. Dua, *Biomed. Pharmacother.*, 2019, **109**, 1249–1258.
26 A. H. Sabri, J. Ogilvie, K. Abdulhamid, V. Shpadaruk, J. McKenna, J. Segal, D. J. Scurr and M. Marlow, *Eur. J. Pharm. Biopharm.*, 2019, **140**, 121–140.
27 Q. Zong, R. Guo, N. Dong, G. Ling and P. Zhang, *Drug Delivery Transl. Res.*, 2022, **12**, 973–980.
28 R. Jamaledin, C. K. Y. Yiu, E. N. Zare, L. N. Niu, R. Vecchione, G. Chen, Z. Gu, F. R. Tay and P. Makvandi, *Adv. Mater.*, 2020, **32**, e2002129.
29 Y. Zhang, H. Hu, Q. Jing, Z. Wang, Z. He, T. Wu and N. P. Feng, *Pharmaceutics*, 2020, **12**.
30 Y. Huang, H. Lai, J. Jiang, X. Xu, Z. Zeng, L. Ren, Q. Liu, M. Chen, T. Zhang, X. Ding, C. Zhao and S. Cui, *Asian J. Pharm. Sci.*, 2022, 679–696.
31 L. Zhang, R. Guo, S. Wang, X. Yang, G. Ling and P. Zhang, *Int. J. Pharm.*, 2021, **604**, 120749.
32 M. Wu, T. Xia, Y. Li, T. Wang, S. Yang, J. Yu, Q. Liang, T. Shen, M. Yu and B. Zhao, *Asian J. Pharm. Sci.*, 2022, **17**, 284–297.
33 J. Lee, S. H. Park, I. H. Seo, K. J. Lee and W. Ryu, *Eur. J. Pharm. Biopharm.*, 2015, **94**, 11–19.
34 J. S. Kochhar, S. Zou, S. Y. Chan and L. Kang, *Int. J. Nanomed.*, 2012, **7**, 3143–3154.
35 A. GhavamiNejad, J. Li, B. Lu, L. Zhou, L. Lam, A. Giacca and X. Y. Wu, *Adv. Mater.*, 2019, **31**, e1901051.
36 F. Cilurzo, P. Minghetti and C. Sinico, *AAPS PharmSciTech*, 2007, **8**.
37 C. Zhou, C. Sheng, L. Gao, J. Guo, P. Li and B. Liu, *Chem. Eng. J.*, 2021, **413**.
38 J. Guo, Q. Xu, R. Shi, Z. Zheng, H. Mao and F. Yan, *Langmuir*, 2017, **33**, 4346–4355.
39 N. Padmavathy and R. Vijayaraghavan, *Sci. Technol. Adv. Mater.*, 2008, **9**, 035004.
40 K. M. Reddy, K. Feris, J. Bell, D. G. Wingett, C. Hanley and A. Punnoose, *Appl. Phys. Lett.*, 2007, **90**, 2139021.

 This journal is © The Royal Society of Chemistry 2023